Journal of Directed Energy, **1**, Spring 2004, 161–170

Investigation into Laser Beam Correction Through Unsteady Flowfields

Richard S. St. John,* Donald J. Link,† and Barry Foucault‡

Science Applications International Corporation, Jupiter, Florida 33477

Mike I. Jones§ and Erich E. Bender¶

Lockheed Martin Aeronautics Company, Fort Worth, Texas 76101

Time-varying unsteady aircraft flowfields can seriously distort propagating high-energy laser (HEL) beams. Computational fluid dynamic (CFD) codes have matured sufficiently to accurately calculate time-resolved unsteady flow properties for airborne HEL system installations. Aero-optical postprocessing software that calculates wavefront errors from unsteady CFD predictions has also been developed and interferometrically validated. These codes may be utilized to derive stroke, bandwidth, and modality requirements for adaptive optic (AO) systems needed to correct time-varying flowfield aberrations and maximize HEL target irradiance. Aero-optic wavefront error maps from unsteady flowfields surrounding an HEL turret at realistic flight conditions were generated by Lockheed Martin Aeronautics Company. Science Applications International Corporation, using the aforementioned wavefront error maps, utilized an idealistic AO system to examine AO requirements for airborne HEL beam correction. A Hartmann wavefront sensor (WFS) and deformable mirror (DM) combination was used for higher order wavefront error correction and a tracker and fast-steering mirror combination for tilt correction. Temporal outputs of original and residual wavefront errors, Zernike coefficients, DM commands, WFS outputs, and Strehl analyses, as well as derived AO system requirements, are given for various WFS subaperture fields of view and for various DM and fast-steering mirror control bandwidths.

KEYWORDS: Adaptive optics, Aero-optics, Unsteady flowfield aero-optics wavefront errors

1. Introduction

Aerodynamic flowfields surrounding tactical fighter aircraft can seriously disrupt performance of high-resolution visible/IR imaging and tracking systems, high-energy laser (HEL) weapon lethality, and beacon beams for wavefront error (WFE) measurement. Both steady and unsteady fighter flowfield properties can be predicted to useful accuracy using

Received February 11, 2003; revision received May 15, 2003.

*Staff Scientist, Lasers, Optics, and Imaging. Member DEPS. Corresponding author; e-mail: stjohnr@saic.com.

†Senior Scientist, Lasers, Optics, and Imaging. Member DEPS.

‡Senior Scientist, Lasers, Optics, and Imaging.

§Technical Fellow, Optical/Directed Energy/Signature Technologies. Corresponding author; e-mail: michael.i.jones@lmco.com.

¶Senior Specialist, Aerodynamics and CFD.

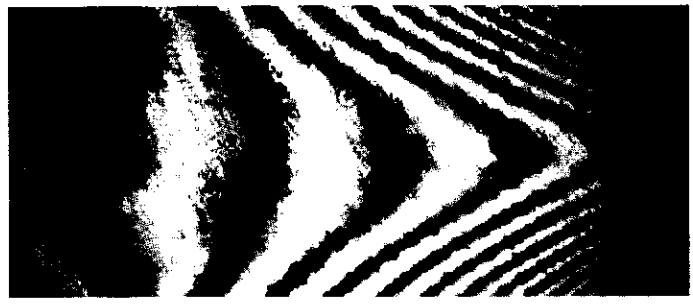

Fig. 1a. Measured double-pass Fizeau interferogram at 532-nm wavelength.

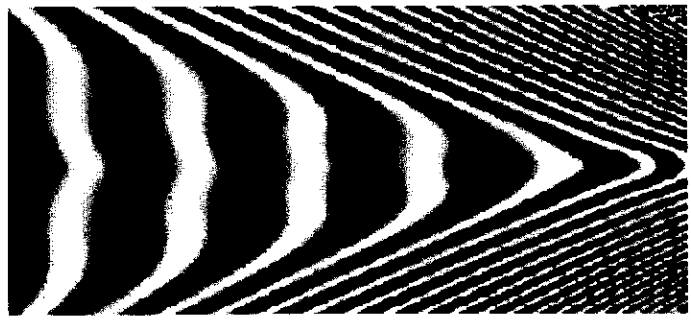

Fig. 1b. Interferogram calculated from CFD.

computational fluid dynamics (CFD) codes such as the Lockheed Martin FALCON and SPLITFLOW codes. Jones and Bender[1] developed FALCON/SPLITFLOW-based aero-optical raytrace codes for calculation and postprocessing of optical transmitted wavefronts through steady and unsteady flowfields. These codes were validated in the summer of 2000 using double-pass Fizeau interferometry in wind tunnel testing at several test conditions and flow velocities up to Mach 4, achieving agreement to within 1/4 wave root-mean-square (RMS) at 532 nm over the majority of the 6-in. test aperture. Figures 1a and 1b show the comparison in a 6-in.-path-length snapshot 6.5 in. downstream.

Using these validated CFD-based aero-optic codes, Jones and Bender calculated transmitted WFEs for an unfaired upper 10-in.-aperture turreted beam director at 1.064 μm using 20-μs CFD solution steps spanning 0.14 s of unsteady flow analysis. Flight conditions were 20-kft altitude, Mach 1.2, and 0-deg angle of attack. WFEs for six beam shafts at varying azimuth and elevation angles, shown in Fig. 2, were analyzed for time-varying X-tilt, Y-tilt, defocus, and tilt-removed RMS WFE components. Temporal analysis of these components gave an insight to the stroke and modality requirements needed by the adaptive optics (AO) system to correct each beam. Frequency analysis revealed spectral energies for these components, which directly drive AO closed-loop bandwidth and latency requirements.

The turret geometry analyzed by Jones and Bender[1] is a simplified representation of current directed energy concepts for tactical aircraft and was used to demonstrate the magnitude of undesirable unsteady flowfield effects on optical beam quality. In particular, a 22-in. pop-up turret, modeled via a hemisphere atop a cylinder, was placed 15.5 ft behind the nose of a 42-ft-long fuselage. No attempt was made to optimize the aerodynamic integration for this

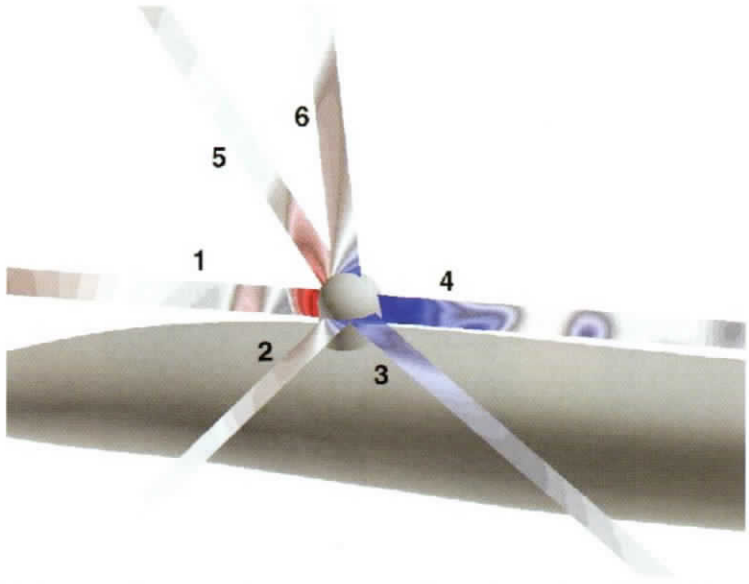

Fig. 2. Six HEL beam shafts analyzed with unsteady flow CFD analysis.

model. Such analyses can also be used to evaluate the effectiveness of flow control methods for reducing these unsteady effects.

The study clearly showed the presence of several distinct regions for HEL beam pointing. Forward-pointing beams suffer significant steady-state aero-optic aberrations that do not vary appreciably with time. Beams aimed through the three-dimensional (3D) flow separation zone around the turret have two fairly distinct look-direction dependent pupil partitions, one having significant but steady aberrations and the other having even more severe aberrations that vary strongly with time. This behavior poses particularly difficult requirements for deformable mirror (DM) stroke and bandwidth. Aft-pointing beams are completely immersed in regions of extreme flowfield density fluctuation and have very strong time-varying aberrations. Aft-pointing beams pose the most stressing correction requirements on AO systems.

From Jones and Bender's analysis,[1] and presented in Fig. 3, it is shown that beam 1 suffers only moderate higher order degradation. WFE correction in this case is rather straightforward. On the other hand, since beams 3 and 4 are propagated through the unsteady flow region, large higher order WFEs are present. These errors, in the worst case, may exceed 12 wavelengths peak-to-valley with more than two waves of RMS error.[1]

Further analysis shows significant tilt components in all the beam paths: as large as 200 waves.[1] This being the case, in order to tilt-correct these WFEs, a tracker with an ample field of view must be used. Likewise, each wavefront sensor (WFS) must also have sufficient field of view in order to curtail cross talk.

Defocus is another strong contributing factor to the large WFEs. The method used for this paper was to let the DM correct for the defocus directly. It should be noted that another, offloading defocus to primary/secondary combination or modal mirror might perform better.

Another complexity to conquer will be correcting the temporal components of the WFEs. Frequency analysis shows strong tilt, defocus, and RMS WFE modes as high as 500 Hz

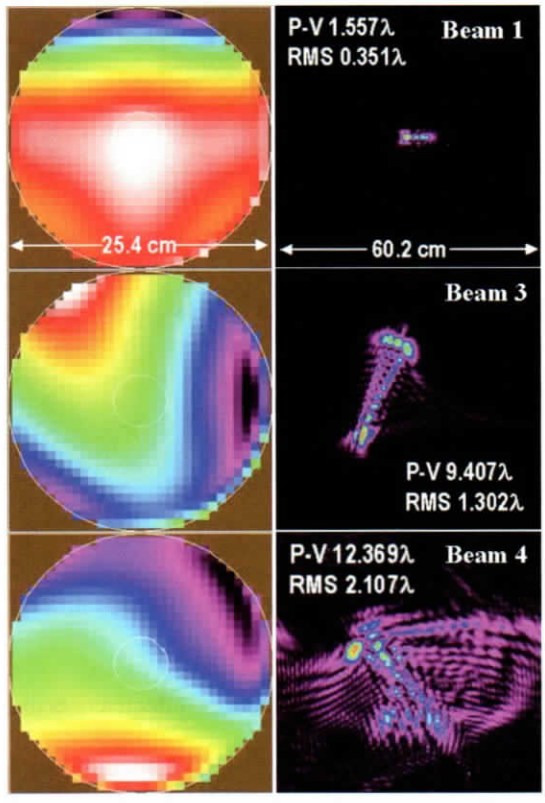

Fig. 3. Representative WFE and laser burn patterns for beams 1, 3, and 4.

(Ref. 1) (Fig. 4). For an AO system to be successful in this case, adequate servo bandwidths for the fast steering mirror (FSM) and DM are a must.

2. Simulation Overview

A first-cut at correcting the WFEs for beams 2, 3, and 4 was undertaken in this paper. A simple, idealistic AO system was designed, set up, and simulated using the code Atmospheric Compensation Simulation (ACS). ACS is a well-anchored, time-domain wave optics simulation primarily used to investigate the effectiveness of AO systems for correcting optical aberrations due to atmospheric turbulence, thermal blooming, and the optical system and resonator. However, our configuration consisted only of a tracker/FSM combination for tilt control working in concert with a WFS/DM pair for higher order WFE corrections (Fig. 5). Moreover, the wave optics propagations were done in a vacuum, meaning there were no atmospheric aberrations, no absorption and scattering, no scintillation, no thermal blooming, etc. Huge WFEs necessitated the use of large propagation grids: 2048 × 2048 with 800 grid points across the clear aperture. A point source, at a wavelength of 1.06 μm, was propagated from the far field through the 10-in.-diameter primary mirror, at which phase screens generated from the optical path difference (OPD) maps of beams 2, 3, and 4

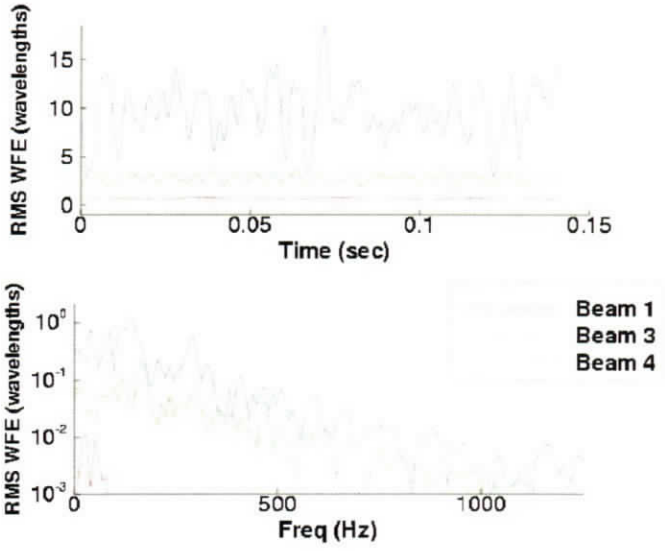

Fig. 4. WFE frequency analysis for beams 1, 3, and 4.

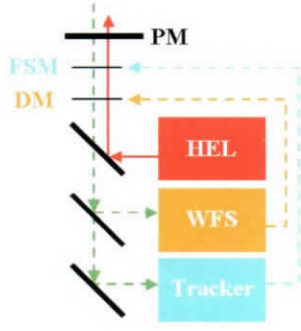

Fig. 5. AO schematic.

were updated at a rate of 100 Hz and then temporally interpolated to match the simulation frame rate. The resulting aberrated wavefront was corrected by the DM and FSM and then passed to subroutines that simulate the WFS and tracker. The outputs from these sensors drove the DM and FSM using standard algorithms. It is also important to note that the DM was free to move without limits. In particular, actuator stroke limits and interactuator stroke limits were not implemented.

The simulation ran for a 0.3-s engagement. Scoring starting after 0.01 s. The figures of merit were far-field Strehl ratios. They were computed by propagating the HEL through the optical beam train to the far field, which was 20 km in this case.

2.1. Tilt Correction

Tilt correction was accomplished using a tracker/FSM combination. The tracker was modeled via a noise-free, 256 × 256 pixel focal plane with a 1.536-mrad total field of view. Three different tracker update frame rates were used: 1, 5, and 10 kHz. The FSM was a flat

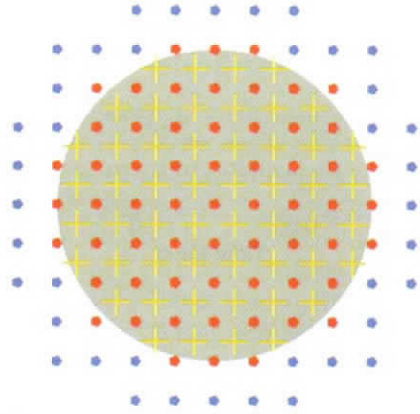

Fig. 6a. 8×8 WFS/DM configuration.

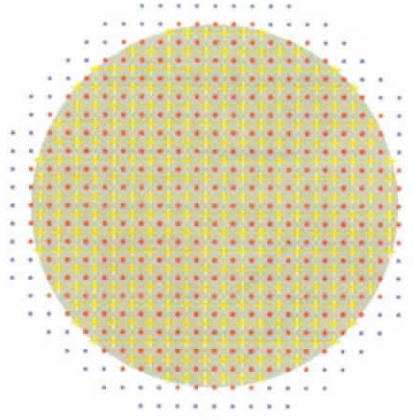

Fig. 6b. 20×20 WFS/DM configuration.

mirror with a servo bandwidth set to 10% of the tracker frame rate. Both the DM and FSM suffered 1 frame of latency.

2.2. Higher Order WFE Correction

Two noise-free Hartman WFS configurations were used (Figs. 6a and 6b). Red and blue dots represent active and slaved actuators, respectively, and the gold pluses denote the center of the subaperture. In both cases, the WFS update rates match the tracker frame rates: 1, 5, and 10 kHz. Similarly, the DM servo bandwidth was 10% of the WFS frame rate. The fields of view of the WFS subapertures were varied from 8 to 32 μrad to account for the large localized tilt. To accomplish this, the number of pixels per subaperture was increased, keeping each pixel's field of view equal to 1 wavelength per subaperture diameter. Centroid offsets were computed using all subaperture pixels. These centroid offsets were then processed to reconstruct the conjugate of the aberrated wavefront by sending commands to poke the DM actuators.

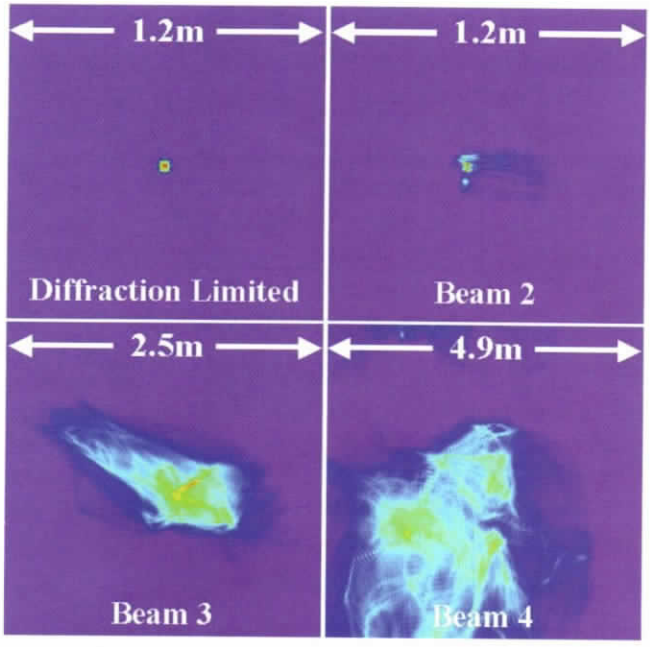

Fig. 7. Open-loop accumulated irradiance profiles.

3. Results

Figure 7 shows the open-loop accumulated irradiance profiles. Computing a point-wise running average of the irradiance values in the calculation grid generated these profiles. The diffraction limited peak irradiance is used as a normalization factor to compute Strehl ratios. That is, an unaberrated wavefront was propagated to the far field, and the peak irradiance was found. Similarly, the peak irradiance is found for the aberrated beam. The resultant ratio of aberrated irradiance over diffraction-limited irradiance is called the Strehl ratio. Clearly then, perfect performance has a Strehl ratio of 1.0 and declines as performance declines.

Two Strehl ratios were considered as the figure of merit. The first is the short-term peak Strehl (STP). The STP ratio is the temporal average of the instantaneous peak Strehl ratio. The other is a time accumulated peak Strehl ratio or long-term peak Strehl ratio (LTP). For the accumulated Strehl ratio, irradiance profiles are accumulated temporally and the resultant peak is located and used in the Strehl calculation.

WFS/DM configurations, AO control bandwidths, and WFS fields of view were the factors modified to test the effectiveness of the AO system.

3.1. Beam 2 Clean-Up

The line of sight for beam 2 was pointing 45 deg forward into the line of flight.[1] Airflow in that region generates WFEs that are easily corrected. This claim is verified by viewing the open-loop accumulated irradiance profile. System performance data are shown in Fig. 8. As expected, the beam clean-up for the 20×20 WFS configuration was very good and was not affected very much either by WFS field of view or by closed-loop control bandwidths.

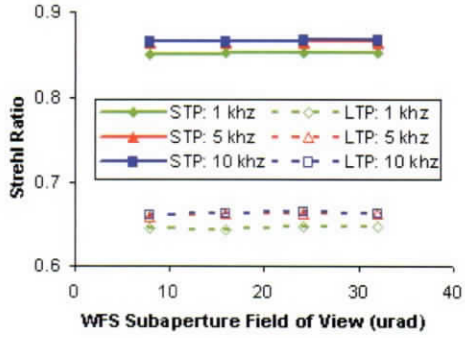

Fig. 8a. AO system performance for beam 2 using the 20 × 20 WFS configuration.

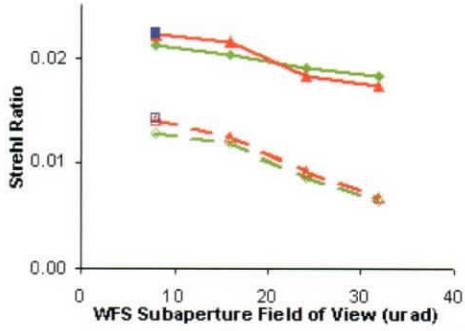

Fig. 8b. AO system performance for beam 2 using the 8 × 8 WFS configuration.

However, beam clean-up with the 8 × 8 WFS was extremely poor. Furthermore, since the 8 × 8 WFS/DM combination failed to correct the weakest turbulence, it certainly will not be able to correct the larger aberrations. So, it is concluded here that the 8 × 8 configuration is not sufficient, and no further analysis will be given.

3.2. Beam 3 Clean-Up

The line of sight for beam 3 was rotated 135 deg behind the turret. Large WFEs exist because the line of sight was partially in the turret wake. Figure 7 shows a much worse open-loop accumulated irradiance pattern and as a result, beam clean-up was expected to be more difficult. Contrary to beam 2, both WFS field of view and control bandwidth had an effect on system performance. It became clear (Fig. 9) that system performance improvements were affected more by closed-loop control bandwidths than by WFS field of view. This was not surprising since frequency analysis of beam 3 showed strong higher-order WFE modes as high as 500 Hz (Ref. 1). FSM and DM control bandwidths of 100 Hz were not sufficient. More analysis needs to be done to find optimal control bandwidths.

3.3. Beam 4 Clean-Up

Directly behind the turret, in the turret wake, are the most significant turbulent airflow and wavefront errors. Beam clean-up there was very difficult indeed. Analysis here showed

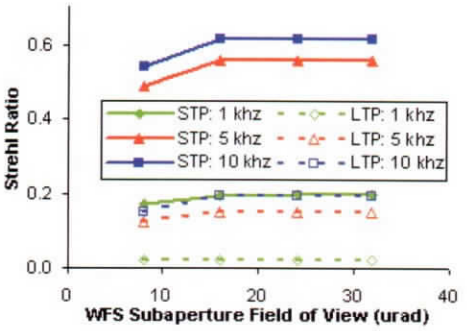

Fig. 9. AO system performance for beam 3 using the 20 × 20 WFS configuration.

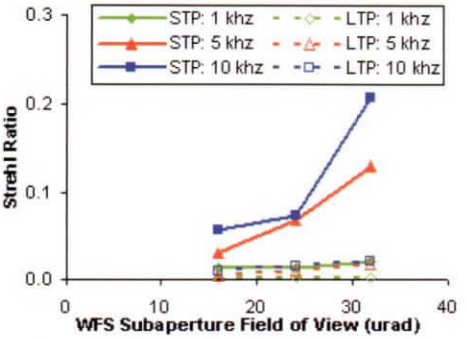

Fig. 10. AO system performance for beam 4 using the 20 × 20 WFS configuration.

overall system performance of much less than 1% accumulated peak Strehl and a STP ratio ranging from 5% to 20% (Fig. 10). This is likely not sufficient for most tactical scenarios. Despite the poor results here, it is possible that a more aggressive system can be conceived to improve performance and should be considered.

4. Conclusions

Using ACS to simulate an ideal AO system's ability to correct WFEs generated by aircraft flowfields and wakes, we have seen that sufficient beam clean-up is possible for a large range of look-angles from the turret. Now, a more realistic AO system that includes atmospheric conditions, hardware emulations, and target/platform interactions should be considered to see whether the results presented here hold true.

Looking directly behind the turret, through the turbulent airflow, generated WFEs that were extremely difficult to correct. While the designed system failed to provide sufficient correction, it may be possible to design a system that does. Two factors lead to this statement. First, some correction was obtained for the aft-pointing beam. Second, flow control methods will help to reduce the wake turbulence. Coupling these factors may produce a result similar to beam 3. In any event, more analysis is required to determine whether a more realistic system will yield adequate performance.

Reference

[1]Jones, M.I., and E.E. Bender, "CFD-Based Computer Simulation of Optical Turbulence Through Aircraft Flowfields and Wakes," AIAA Paper 2001-2798, 2001.